

Exploring Parameter Spaces in Dynamical Systems

Christian Kuehn

Abstract

The parameter space of dynamical systems arising in applications is often found to be high-dimensional and difficult to explore. We construct a fast algorithm to numerically analyze “quantitative features” of dynamical systems depending on parameters. Using a classical problem from mathematical ecology as an example, we demonstrate how to apply the algorithm to investigate the amplitude of a limit cycle depending on seven parameters. We stress the practical value of the algorithm but we also provide a rigorous error analysis to justify the overall strategy. Our approach turns out to be particularly useful in the case of comparing experimental data to a model defined by differential equations and to investigate whether the equations can approximate the modeled system.

1 Introduction

In this paper we investigate the problem of how to explore parameter spaces for dynamical systems. We shall focus on ordinary differential equations (ODE), but remark that our approach works also in different settings such as difference equations, partial differential equations or stochastic dynamics

Parametrized dynamical systems in mathematical modelling not only lead to questions about structural features of the model and their dependence on parameters, which is the is central question in applied bifurcation theory, but also to quantitative questions. The main question we are going to address is how a feature, like a limit cycle or a homoclinic orbit, depends on parameters. Some questions often encountered are:

- What is the amplitude of a limit cycle?
- What is the time required to traverse a part of a homoclinic orbit?
- How far does an invariant manifold extend in phase space?

All answers are obviously parameter dependent and are going to have relevant interpretations in the modelling problem under consideration. Drawing quantitative conclusions requires understanding how different parameters influence the feature. Even if the parameter space is of moderate dimension ($\approx 15 - 25$ parameters) it is often infeasible to numerically explore it systematically by computing a dense grid of parameters values. In many mathematical models no dedicated techniques are used to explore the parameter space. Instead several “ad-hoc” methods are used which can potentially yield incorrect conclusions.

Most existing techniques for exploring parameter spaces systematically are based on purely statistical methods and in particular on sensitivity analysis. A short exposition of the methods of sensitivity

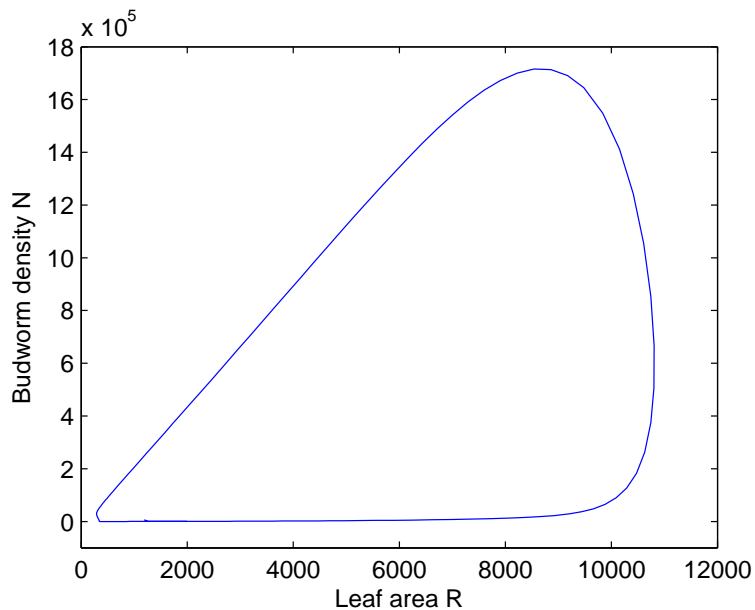


Figure 1: Limit cycle at default parameters given in Table 1

analysis can be found in [11]. A detailed explanation of several advanced ideas is given in [10]. Our algorithm parallels one of the approaches from sensitivity analysis by using a Monte-Carlo type method. However, the key difference between our approach and known methods is that we take advantage of the vector field “directly” in computations to find a more efficient algorithm. In particular, we are not interested in a black-box scheme which works for all mathematical models, but to design a method which uses the structure of the model given by a continuous or discrete-time dynamical system.

2 Limit Cycles in ODEs - The Spruce Budworm

We use a classical example from mathematical ecology to illustrate our algorithm. The 2-dimensional ODE model proposed in [7] represents the interaction between the spruce budworm N and the leaves of a forest R . It is a simplification of a 3-dimensional system for the same ecological situation given in [6]. The paper [6] is partly based on earlier work in [5], whereas re-expositions of the spruce budworm model can be found in many textbooks by now (see e.g. [13]). Our model reads:

$$\begin{aligned} \dot{R} &= p_1 R \left(1 - \frac{R}{p_3}\right) - p_7 N \\ \dot{N} &= p_2 N \left(1 - \frac{N}{p_4 R}\right) - p_5 \frac{N^2}{p_6^2 R^2 + N^2} \end{aligned} \quad (1)$$

where R is the branch area and N is the budworm density. To keep the notation simple we deviate from the conventions in ecology and simply index the seven parameters p_1, \dots, p_7 .

The descriptions, units and default values are summarized in Table 1. We consider the model only for $R, N \geq 0$ representing biologically sensible nonnegative quantities.

Table 1: Parameters for the sample problem

Parameter	Description	Units	Default Value
p_1	intrinsic branch growth rate	1/yr	0.15
p_2	intrinsic budworm growth rate	1/yr	1.6
p_3	maximum branch density	branches/acre	24000
p_4	maximum budworm density	larvae/branch	200
p_5	maximum budworm predated	larvae/(acre*year)	28000
p_6	half of maximum density for predation	larvae/branch	1.5
p_7	consumption rate of budworm	(branches*acre)/(yr*larvae)	0.0015

We investigate the characteristics of a hyperbolic limit cycle $\gamma \subset \mathbb{R}_+^2$, which represents long-term coexistence for branches (i.e. trees) and the budworm population. A stable limit cycle occurs at the given default parameters (see Figure 1). We observe from equation (1) and Table 1 that the variable R is slow compared to the variable N . This means that (1) is a slow-fast system. Direct calculation of the nullclines shows that the observed limit cycle is a relaxation oscillation.

For equation (1) we have to explore a 7-dimensional parameter space. We denote the parameter space by $P \subset \mathbb{R}_+^7$ and an element in P by $p = (p_1, \dots, p_7)$. To indicate the dependence of γ on p we shall also refer to the limit cycle as $\gamma(p)$.

Biologically relevant questions are to find the maximum values of the coordinates of $\gamma(p)$. These values correspond to the maximum branch area $R_{max}(\gamma(p))$ and maximum budworm density $N_{max}(\gamma(p))$ along a cycle. The maximum budworm density is particularly important as it describes the maximum insect outbreak in the ecosystem. Our main focus is to find the directions in P which correspond to relevant variations of $R_{max}(\gamma(p))$ or $N_{max}(\gamma(p))$. Notice that our aim is to determine parameter dependencies globally as well as locally, i.e. we are interested in the overall behaviour as well as significant variations around points. A further goal is to identify functional dependencies of $R_{max}(\gamma(p))$ or $N_{max}(\gamma(p))$ on subsets of parameters to distinguish between a linear and a nonlinear response.

3 An Algorithm for Parameter Space Exploration

We are going to describe the algorithm in the general setup of ODEs and illustrate all steps with the model given by equation (1).

3.1 The Setup

Consider an ordinary differential equation

$$\dot{x} = f(x, p) \quad \text{for } x \in \mathbb{R}^n, p \in P \subseteq \mathbb{R}^k \text{ and } f \in C^1(\mathbb{R}^{n+k}) \quad (2)$$

where p is a vector of parameters $p = (p_1, p_2, \dots, p_k)$. Suppose that equation (2) has a quantitative property $\gamma(p)$ such as a limit cycle (or e.g. a heteroclinic orbit). By “quantitative” we refer to the possibility of measuring an important characteristic of $\gamma(p)$ like cycle amplitude (or e.g. length of a

heteroclinic connection). Furthermore assume that we have a compact set $B \subseteq P$ in which the feature is persistent, i.e. we do not have any bifurcation points inside B . We shall refer to B as a hyperbolic domain for $\gamma(p)$.

Define a function $C : B \rightarrow \mathbb{R}$ given by mapping a parameter vector p to $C(p)$, where $C(p)$ is the quantitative measure of $\gamma(p)$. Assume we have a method to compute C numerically. Notice that C might be very expensive to compute as a single function evaluation usually requires at least one complete numerical solution of equation (2).

In our sample problem we take $B = \{p_i^{default} \pm \delta_i\} \subseteq \mathbb{R}_+^7$ where δ_i are chosen based on the combinations and ranges of parameters we are interested in and to preserve the limit cycle $\gamma(p)$ found in the first quadrant for the default values given in Table 1. If we compute $\gamma(p)$ numerically we obtain a finite sequence of values $(\gamma(p)_{R,k}, \gamma(p)_{N,k})$, where the indices ‘‘R’’ and ‘‘N’’ denote the coordinate directions in (1). If we are interested in the maximum insect outbreak we define $C(p)$ by

$$C(p) = \max_k \gamma(p)_{N,k} \quad (3)$$

Defining $C(p)$ obviously depends on the given problem and the questions of interest in the mathematical model.

3.2 Discretization

Assume without loss of generality that B is connected; if this is not the case we can compute for each of the components of B separately. Choose a finite grid $G \subset B$ of spacing s_i in direction p_i defined by intersecting a scaled lattice with B so that

$$G = \{(s_1 \cdot \mathbb{Z}, s_2 \cdot \mathbb{Z}, \dots, s_k \cdot \mathbb{Z}) \in \mathbb{R}^k\} \cap B \quad (4)$$

Note that we have chosen the lattice to be uniformly spaced in each direction. This is not necessary for any of the following calculations. We should change to a nonuniform grid if there is a priori information about parameter regions available having large variations in $C(p)$. In our model problem we have chosen a uniform spacing in each direction.

Now consider the graph formed from G by connecting all points which differ in one coordinate p_i by precisely s_i . We also use G to denote this graph. Metrize G by

$$d(p, q) = \text{minimum number of edges connecting } p \text{ to } q \quad (5)$$

3.3 Relevance Measure

The next step is to compare two given elements $p, q \in G$ and estimate when $|C(p) - C(q)|$ is ‘‘large’’. To do this we use the given vector field f . In the following we shall describe the most basic version of the procedure.

Step 1: Select a set of points in phase space determined by $\gamma(p)$. This is best illustrated by a concrete example. For our limit cycle γ we can choose k_1 different parameter values. We compute γ for each parameter value and we select m points in phase space on the computed limit cycle. This gives a collection of points in phase space:

$$S_x := \{x_i \mid i = 1, 2, \dots, k_2 = mk_1\} \quad (6)$$

We choose k_1 and m such that the number of elements in S_x is small. In our model problem we have computed γ for a set of values chosen uniformly at random from G with $k_1 = 4$. Then we selected $m = 4$ points on each computed limit cycle starting with a random point and uniform spacing along the cycle. This gives a sample representing the different shapes of possible cycles in phase space.

Step 2: Choose a set points from parameter space

$$S_p = \{p^1, p^2, \dots, p^{k_3}\} \subset G \quad (7)$$

uniformly at random. Fix a neighbourhood size in G , i.e. pick an integer n_{size} such that a neighbourhood of a point p is given by $\Omega_p = \{q \in G | d(q, p) \leq n_{size} \text{ and } q \neq p\}$. For each value $p^j \in S_p$ choose a fixed number of neighbours k_4 at random from Ω_{p^j} , call this set S_{p^j} ; usually we want to pick between k_4 between 2 and 4, but any number less than the number of elements in Ω_p is possible. In preparation for the next step, we mention that we should choose $\#(S_p) = k_3$ such that a summation of $k_4 \cdot k_3 \cdot k_2$ elements is computationally feasible.

Step 3: Estimate a measure of relevance. Again we consider the model problem for illustration. Let

$$r = \frac{1}{k_2 k_3 k_4} \sum_{j=1}^{k_3} \sum_{q \in S_{p^j}} \left| \sum_{i=1}^{k_2} (\|f(x_i, p^j)\|_2 - \|f(x_i, q)\|_2) \right| \quad (8)$$

So r represents the average variation between two neighbours along the sampled points and hence can be taken as an estimator for the variation of the limit cycle from one point to a neighbouring point. Hence we have found a way to estimate when $|C(p) - C(q)|$ is “large”. We call r the (average) relevance measure. We can also define

$$M(p) = \frac{1}{k_2} \sum_{i=1}^{k_2} \|f(x_i, p)\|_2 \quad (9)$$

which we refer to as the relevance function. We can easily compute the relevance function for different values of p as we only need a small number of evaluations of the vector field if S_x is small. We shall discuss more advanced methods of defining r and $M(p)$ in Section 4.

3.4 Neighbour Comparison

Let $p, q \in G$ be given in parameter space and suppose we have already computed $C(p)$. Now we choose a neighborhood Ω_p of p in G excluding p itself, e.g. $\Omega_p = \{q \in G | d(p, q) = 1\}$. Fix a tolerance $tol \in [0, \infty)$, then the rationale for approximating the desired function C is:

- If $q \in \Omega_p$ and $|M(p) - M(q)| \geq tol \cdot r \Rightarrow q$ shows a relevant variation so we compute $C(q)$
- If $q \in \Omega_p$ and $|M(p) - M(q)| < tol \cdot r \Rightarrow q$ does not show a relevant variation so set $C(q) = C(p)$

Clearly we have two special cases:

- $tol = 0$: In this case we always compute any point encountered by the algorithm exactly.
- $tol = 1 + \max_{p, q \in G} |M(p) - M(q)|$: In this case we never compute any neighbours of points and just set their values to be the value of the center p .

In our model problem we used the criterion for several values of tol between 0.9 and 1.1. The reason for comparing with neighbours will be explained in sections 3.6 and 3.7.

3.5 Iteration

We describe next how to run the exploration algorithm to compute $C(p)$. We have two choices to proceed:

1. Fix a subset G_0 of G , for each point $p \in G_0$ compute $C(p)$. Fix a neighbourhood size for each point such that neighbourhoods of points in G_0 do not intersect and perform neighbourhood comparisons and computations as described in section 3.4. We call this method deterministic exploration.
2. Start with a random initial point $p \in G$. Compute $C(p)$ and mark p as checked. Consider a neighbourhood Ω_p and perform neighbourhood comparisons and computations as described in section 3.4 for all neighbours which have not been marked yet. Mark all elements in Ω_p . Now choose a new random point out of all unmarked points. We call this method (uniform) random exploration.

For both methods we can choose a fixed number of points i_{max} , which should be explored. Clearly i_{max} should be defined so that $i_{max} \leq \#(G)$. Having reached i_{max} we have obtained the function C on a subset G^* of the grid G . Notice that if the grid size shrinks to zero and i_{max} approaches $\#(G)$ the algorithm converges to a full computation of C .

The most successful algorithms for higher-dimensional numerical problems often use an element of randomization. A classical example is numerical integration. In this area Monte-Carlo techniques are predominant for any problems of dimension > 4 (see e.g. [2] for a survey). Hence we expect the deterministic exploration to work only for small number of dimensions and recommend the random exploration.

3.6 Interpolation

Given the values of C on G^* we obtain all values in the hyperbolic domain B by interpolation. This constructs C on the full domain B . For our model problem we used linear interpolation. For details on basic numerical methods for interpolation consider [3]. Most algorithms currently in use for multi-dimensional interpolation are based on a Delauney triangulation of given data. Many use the 'quick hull'-algorithm (QHULL, see [1],[8]); we used the version of QHULL implemented in MatLab for our sample problem.

One reason why we have used neighbour comparison as described in section 3.4 is obvious from the one-dimensional toy-example illustrated in Figure 2. Independent of all previous considerations, just suppose the 1-dimensional interpolation problems on $[0, 1]$ are:

$$\begin{aligned} &\{(0, 0.3), (0.5, 0.25), (1, 0.3)\} \quad \text{Problem 1} \\ &\{(0, 0.3), (0.5, 0.25), (0.58, 0.04), (1, 0.3)\} \quad \text{Problem 2} \end{aligned}$$

One extra point gives the indication that there is a relevant decrease of the function value to the right of 0.5 whereas no neighbour comparison would entirely miss this decrease. This means that the local comparison helps us to detect globally important directions of variation of $\gamma(p)$, which could be missed just using point-wise Monte-Carlo exploration without neighbour comparison. It also indicates directions which are of interest near a point. We refer to this feature of our method as local/global

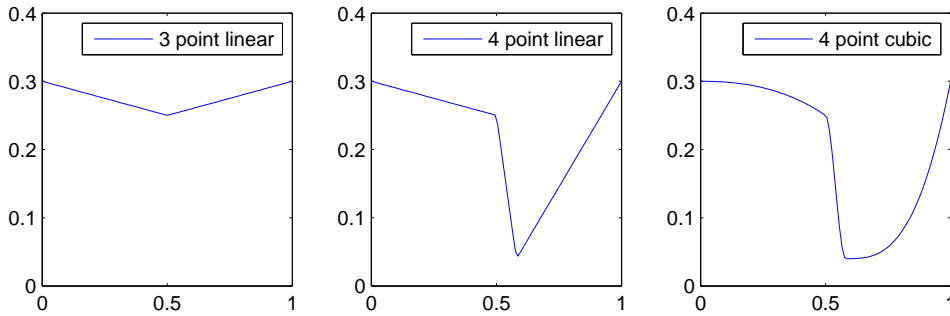


Figure 2: Interpolation for 3 points linear, 4 points linear and 4 points cubic spline

approximation.

Furthermore we see that other interpolation methods, such as the cubic spline in Figure 2, work as well, but might introduce a functional dependence due to the interpolation method. Therefore the conservative approach is to use linear interpolation and investigate interesting regions in parameter space more closely once a significant decrease or increase in the function C is found.

3.7 Results and Visualization

To determine the influence of parameters on the structurally stable feature $\gamma(p)$ we have to organize the output of the previously described steps, i.e. we can either work with a subset of values G^* or its interpolation to the hyperbolic domain B . Some problems arising are:

- Are there “enough” points to perform interpolation on B or on some given subset of B ?
- How to visualize the output of high-dimensional data?

We shall not discuss the two questions in detail as they form subjects on their own and just focus on a few special issues.

The method of neighbour comparison balances the effect of dimension with respect to the number of points necessary for interpolation. Consider our model problem and suppose we fix five parameters on G^* and want to interpolate $C(p)$ over the remaining two parameters, i.e. over a 2-dimensional “slice” of B . Using just Monte-Carlo simulation without neighbour comparison will inevitably lead to many slices, which do not have any points on them. With neighbour comparison, by possibly increasing the neighbourhood size, we can assure that we have enough points to perform interpolation. Note that higher-dimensional interpolation techniques can also fail if there are too few points. For example, a Delauney triangulation might not be supported by many algorithms for sparse G^* (see [1], [8] and www.qhull.org).

For a k -dimensional parameter space with $G^* \subset \mathbb{R}^k$ we can fix $k - 2$ parameters and plot 3-dimensional output for $C(p)$. This can be achieved by viewing $C(p)$ as a surface over the two variable parameters. We found this method particularly useful coupled to animations, which allow for moving a third parameter and hence produce moving surfaces. During the algorithm we can easily keep track

of points, which have been computed and those, which have been set to a local constant by neighbour comparison. Therefore we are able to identify regions and directions containing relevant variations.

It should be clear that it is also easy to get estimates of maximum and minimum values over G^* and hence over B . For example, in the budworm problem posed in section 2 we can now determine for any given region of parameter space an estimate of the maximum insect outbreak.

3.8 Summary of the Algorithm

The main steps can be summarized as follows:

1. Identify the quantitative feature $\gamma(p)$ and its hyperbolic parameter domain B .
2. Define a quantitative measure of $\gamma(p)$ encoded in a function $C : B \rightarrow \mathbb{R}$.
3. Discretize the space B and define a metric on the discretization G .
4. Sample points from phase space “representing” the feature $\gamma(p)$.
5. Choose a measure (e.g. the norm) to estimate the variation of $\gamma(p)$ from the vector field f .
6. Compute the relevance measure r and setup the relevance function.
7. Choose discrete or random exploration and a size of neighbourhoods for computed points.
8. Define a neighbour comparison based on r and the relevance function.
9. Iteratively compute C on a certain number of points using exploration.
10. Interpolate (linearly) between the values obtained for C .
11. (Visualize and/or evaluate the interpolated function C to explore parameter dependence.)

The overview shows that the algorithm works for other dynamical systems like maps, difference equations or partial differential equations.

4 Advanced Local Exploration

Instead of using the norm of the vector field, we can also use derivatives in the parameter directions, which leads to the relevance measure:

$$r_{\partial} := \frac{1}{k_2 k_3 k_4 k} \sum_{j=1}^{k_3} \sum_{q \in S_{p^j}} \left| \sum_{i=1}^{k_2} \sum_{l=1}^k \left(\left| \frac{\partial f}{\partial p_l}(x_i, p^j) \right| - \left| \frac{\partial f}{\partial p_l}(x_i, q) \right| \right) \right| \quad (10)$$

where we recall that k is the dimension of the parameter space. The corresponding relevance function is given by:

$$M_{\partial}(p) := \frac{1}{k k_2} \sum_{i=1}^{k_2} \sum_{l=1}^k \left| \frac{\partial f}{\partial p_l}(x_i, p) \right| \quad (11)$$

Remark: Using the partial derivatives is a technique employed in local sensitivity analysis and has the potential to produce a better measure of relevance. We can use finite-difference approximations to the derivatives if there is no explicit formula of $f(x, p)$ available. $M_{\partial}(p)$ has the drawback that the computational cost increases.

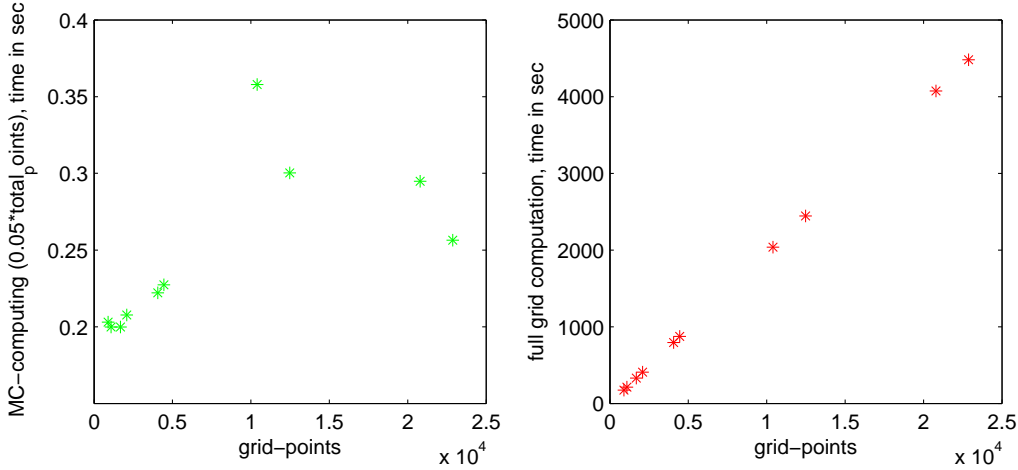


Figure 3: Comparison of computing time for exploration algorithm and full calculation

5 Numerical Results

Note that since equation (1) is a fast-slow system, it is stiff and explicit numerical solvers are going to fail. We used a modified Rosenbrock method of order two with explicitly supplied Jacobian matrix; see [9] for historical reference, [12] for the implementation and [4] for a modern exposition of the Rosenbrock method. We have simulated the system for the following range of parameters:

Table 2: Ranges of parameters for the sample problem - spruce budworm model

Parameter	Default Value	Range	Spacing s_i
p_1	0.15	[0.149,0.151]	0.0001
p_2	1.6	[1.5,1.7]	0.1
p_3	24000	[22000,26000]	250
p_4	200	[190,210]	2
p_5	28000	[24000,32000]	500
p_6	1.5	[1,2]	0.1
p_7	0.0015	[0.001,0.002]	0.0001

The main numerical question to pose is, what computational cost do we save by using our algorithm? This is hard to answer precisely as our goal is to provide a method exploring parameter space, which allows applied researchers to detect the main quantitative dependencies in their models. To perform a practical test we have simulated 10 subsets of the full parameter space grid defined in Table 2. The results of this simulation are shown in Figure 3. We have chosen to use random exploration of five percent of the total number of grid points; together with neighbourhood exploration this yields a sufficiently dense set of values to investigate the function C .

From Figure 3 we observe that the computing time for our algorithm lies between 20 and 40 seconds whereas a full grid computation can take up to 4800 seconds. Now we have to answer the question if we can really extract all the quantitative information we are interested in from our algorithm in

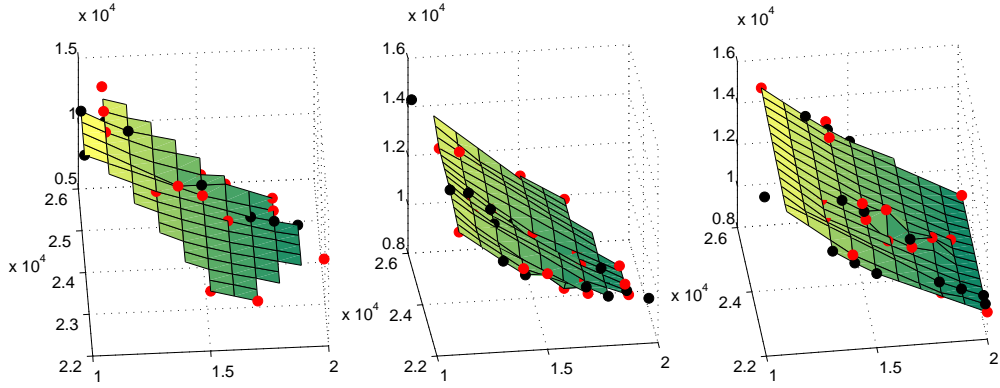


Figure 4: Maximum budworm outbreak as a function of p_3 and p_6 for $p_5 = 24000, 28000, 32000$ - algorithm

comparison to the much slower full grid computation.

Suppose we are interested in the relations between p_3 , p_5 and p_6 . We simulate the system with p_3, p_5 and p_6 in the ranges given in Table 2 and use default values for all other parameters as given in Table 1. We plot the maximum budworm outbreak N_{max} as a function of p_3 and p_6 . Plots for $p_5 = 24000, 28000, 32000$ are shown in Figure 4. The red dots indicate grid points which obtained their values from neighbours. The black dots indicate points which have been fully computed. The computation has been performed with a relevance measure r given in equation (8) and tolerance $tol = 1.1$ (see section 3.4).

Just given Figure 4 we can draw several conclusions: Obviously the outbreak is decreasing with increasing value of p_6 . It is not significantly affected by variations of p_3 compared to p_3 and p_6 . We can see that increasing p_5 decreases the maximum outbreak by comparing among all three figures. The plots show a weakly nonlinear relationship between p_3 and p_6 . We can also conclude that the quantitative feature varies “uniformly” in all three parameter directions, i.e. does not exhibit several nonlinear relationships in our region of interest.

Now let us compare these findings with the computation on the full grid, which is given in Figure 5. We see that all our previous conclusions have been verified by the full computation. The only observation we should make is that the first plot in Figure 4 and Figure 5 do not seem to match well. This results from the fact that our algorithm has produced few values for small p_6 and small values of p_5 so that this region was not interpolated. We could simply remedy this by extending the current interpolation to the boundary but we decided on the most conservative approach given the computed data.

Comparing the computational cost we have computed the two figures on several standard desktop workstations and obtained that it took approximately 10-15 seconds to compute with our algorithm to obtain $N_{max}(p_3, p_5, p_6)$ for the hyperbolic domain B given by the ranges in Table 2. This means we have obtained a local/global approximation to N_{max} on $32 \cdot 16 \cdot 10 = 5120$ points. The computation of a single slice of p_3 and p_6 for a fixed value of p_5 took approximately 45-50 seconds on the same machines, yielding a total time for the same amount of points given by $> 45 \cdot 16 = 720$ seconds. This

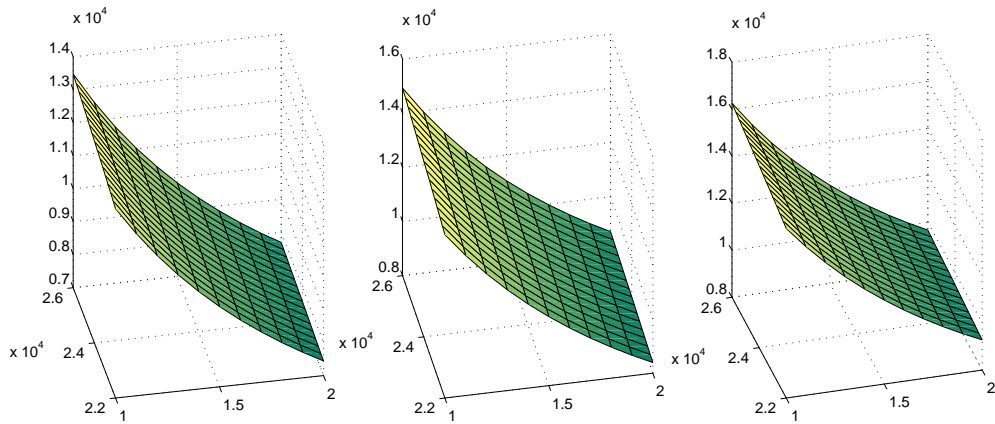


Figure 5: Maximum budworm outbreak as a function of p_3 and p_6 for $p_5 = 24000, 28000, 32000$ - full computation

means that in this practical example we have used only a fraction of the full computation

$$\approx \frac{15}{720} = \frac{1}{48} \quad (12)$$

This 50-fold increase in computation time supplied us with the same conclusions we would have obtained by “brute force”. Notice that this effect increases with dimension.

The computation of a single slice of p_3 and p_6 using our algorithm is about 1 second on most current workstations. This means that we can “move” with 3-dimensional plots through parameter space in real time and adjust the parameters along directions of interest according to the given output.

We have also performed calculations for the full 7-dimensional parameter space and obtained local/global approximations of N_{max} and R_{max} . Although this computation takes around 2 hours for most values of $tol \approx 1$, it is still feasible. We remark that the algorithm can also be ‘scaled’ according to the computational tools available and the desired goals:

- Accurate computations, high computing power, long-waiting time: We decrease tol and select a relatively large fraction of sample points S_x .
- Coarse global estimates, low computing power, direct feedback: We increase tol and reduce the size of S_x .

This means that powerful computing environments can be very useful, but are not necessary to extract reliable information from a model.

6 Error Analysis

The precise error analysis is not the focus of this paper. Nevertheless we shall motivate in this section why we expect an error that behaves like $1/\sqrt{n}$ where n is the number of computed gridpoints.

Assume that the hyperbolic domain B is a compact hyperrectangle. First consider the discretizations $G_j \subset B \subset \mathbb{R}^k$ such that the following condition holds:

$$\min_{p \in G_j} \|p - q\|_2 \rightarrow 0 \quad \text{for all } q \in B \text{ as } j \rightarrow \infty \quad (13)$$

where $\|\cdot\|_2$ denotes the Euclidean norm in \mathbb{R}^k . We call the sequence of grids G_j an approximation sequence for B if condition (13) holds. If $f : B \rightarrow \mathbb{R}$ then we define the usual L^1 norm as:

$$\|f\|_{L^1} = \int_B |f(p)| dp \quad (14)$$

Since B is a compact hyperbolic domain we conclude that $C : B \rightarrow \mathbb{R}$ is bounded (for the definition of the function C , see 3.1). Let $C_A : B \rightarrow \mathbb{R}$ denote the local/global approximation to C obtained by our algorithm for the grid G_j . Recall that we have computed $n(j)$ points (depending on i_{max} and the neighbourhood size) on the grid and used linear interpolation to construct C_A on B ; denote these points by $\{x_k\}_{k=1}^{n(j)}$. Obviously C_A is a random variable depending on the relevance measure r and the grid G_j . Hence we should formally write $C_A = C_{A(r,j)}$, but for simplicity of notation we sometimes just write C_A . Since C is smooth we can modify C_A on the complement of G_j to be piecewise linear and satisfy $C_A(p) > C(p)$ for all $p \in B$.

Let P denote the probability measure on B induced by a uniformly distributed random variable on B . Since B is compact we can assume without loss of generality that $\int_B dx = 1$ so that the density of P is identically 1. Now define

$$I_A = I_{A(j,r)} = \frac{1}{n(j)} \sum_{k=1}^{n(j)} C_A(x_k) \quad (15)$$

We also set $I = \int_B C(p) dp$. This allows us to consider a standard result from Monte-Carlo integration.

Proposition 6.1. *If $tol = 0$ then $C_{A(r,j)} = C_{A(j)}$, i.e. C_A is independent on the random variable r . Suppose $n(j) \rightarrow \infty$ as $j \rightarrow \infty$ then*

$$\frac{I_{A(j)} - I}{\sigma / \sqrt{n(j)}} \xrightarrow{\sim} Z \quad \text{as } j \rightarrow \infty \quad (16)$$

where $Z \sim N(0,1)$, i.e. we have convergence in distribution to a normal distribution with mean 0 and variance 1.

Remark: Note that $j \rightarrow \infty$ implies $n(j) \rightarrow \infty$ even if we only increase the number i_{max} linearly.

Proof. (Sketch, see [2]) If $tol = 0$, no neighbour comparison is performed and all elements are computed, so that C_A is independent of r giving the first result.

Notice that $Var(I_{A(j)})$ is bounded since C is bounded. Then the central limit theorem implies the desired result. \square

For two sequences of random variables $\{X_n\}, \{Y_n\}$ we write $X_n = O_P(Y_n)$ if for any $\epsilon > 0$ there exist $M_\epsilon > 0, N_\epsilon > 0$ such that

$$P\left(\left|\frac{X_n}{Y_n}\right| > M_\epsilon\right) < \epsilon \quad \text{for all } n \geq N_\epsilon \quad (17)$$

so that X_n/Y_n is bounded in probability. Therefore we obtain from Proposition 6.1 that:

$$I_{A(j)} - I = O_P \left(\frac{1}{\sqrt{n(j)}} \right) \quad (18)$$

Since $O_P(\cdot) \approx O(\cdot)$ and $C_A(p) > C(p)$ for all $p \in B$ we can write

$$|I_{A(j)} - I| = \|C_A - C\|_{L^1} = O_P \left(\frac{1}{\sqrt{n(j)}} \right) \approx O \left(\frac{1}{\sqrt{n(j)}} \right) \quad (19)$$

where the last big-oh notation refers to the deterministic asymptotic behaviour on B . We can state the previous discussion as a practical result:

Proposition 6.2. *If $tol = 0$ then $\|C_A - C\|_{L^1} \approx O \left(\frac{1}{\sqrt{n(j)}} \right)$ for $n(j)$ (respectively j) sufficiently large.*

The convergence of the error by an inverse square-root law is obviously very slow. Nevertheless, it is precisely the law we would expect from the use of Monte-Carlo methods. It reflects that we are dealing with a problem without restriction on dimension. Proposition 6.2 justifies our initial claim that we expect an error that behaves like $O(\frac{1}{\sqrt{n}})$.

7 Conclusions

We presented a new algorithmic paradigm to explore the quantitative variation of structurally stable features in dynamical systems depending on parameters. We illustrated our algorithm in the case of ODEs and a 2-dimensional model problem and discussed the main steps of discretization, sampling, relevance measures, neighbour comparison, random exploration and interpolation. Numerical results demonstrate the practical value of our method and its efficiency compared to direct computations. Furthermore, error estimates for the random exploration strategy were proven and confirmed the expected Monte-Carlo type behaviour with error of order $O(1/\sqrt{j})$ independent of the dimension of the phase space or parameter space.

Despite the detailed error analysis, we stress that our primary goal was not to generate accurate data but to provide practioners with a computationally efficient method. The efficiency derives from a strategy which has been very successful in the analytical description of dynamical systems - we do not compute an explicit solution of an equation but characterize its properties directly from the equations and their structure. We have shown that this general idea can be very useful for the numerical investigation of dynamical systems too.

References

- [1] C.B. Barber, D.P. Dobkin, and H.T. Huhdanpaa. The quickhull algorithm for convex hulls. *ACM Transactions on Mathematical Software*, 22(4):469–483, 1996.
- [2] Michael Evans and Tim Swartz. *Approximating Integrals via Monte Carlo and Deterministic Methods*. OUP, 2000.

- [3] Walter Gautschi. *Numerical Analysis*. Birkhaeuser Boston, 1997.
- [4] E. Hairer and G. Wanner. *Solving Ordinary Differential Equations II*. Springer, 1991.
- [5] C.S. Holling. Resilience and stability of ecological systems. *Annual Review of Ecology and Systematics*, 4:1–23, 1973.
- [6] D. Ludwig, D.D. Jones, and C.S. Holling. Qualitative analysis of insect outbreak systems: The spruce budworm and forest. *Journal of Animal Ecology*, 47(1):315–332, 1978.
- [7] R.M. May. Thresholds and breakpoints in ecosystems with a multiplicity of stable states. *Nature*, 269:471–476, 1977.
- [8] J. O’Rourke. *Computational Geometry in C*. CUP, 1994.
- [9] H.H. Rosenbrock. Some general implicit processes for the numerical solution of differential equations. *Computer J.*, 5:329–331, 1963.
- [10] A. Saltelli, K. Chan, and E.M. Scott. *Sensitivity Analysis*. Wiley, 2000.
- [11] A. Saltelli, S. Tarantola, F. Campolongo, and M. Ratto. *Sensitivity Analysis in Practice*. Wiley, 2004.
- [12] L.F. Shampine and M.W. Reichelt. The matlab ode suite. *SIAM Jour. Sci. Comp.*, 18(1):1–22, 1997.
- [13] P. Yodzis. *Introduction to Theoretical Ecology*. Harper & Row, 1989.